Molecular Crystals and Liquid Crystals

ISSN: 1542-1406 (Print) 1563-5287 (Online) Journal homepage: http://www.tandfonline.com/loi/gmcl20

The Preparation and Characterization of New Antazoline Salts with Dicarboxylic Acids

Agnese Dravniece, Andris Actiņš, Kristīne Krūkle-Bērziņa & Inese Sarceviča

To cite this article: Agnese Dravniece, Andris Actiņš, Kristīne Krūkle-Bērziņa & Inese Sarceviča (2015) The Preparation and Characterization of New Antazoline Salts with Dicarboxylic Acids, Molecular Crystals and Liquid Crystals, 606:1, 154-164, DOI: 10.1080/15421406.2014.905041

To link to this article: http://dx.doi.org/10.1080/15421406.2014.905041

Published online: 15 Jan 2015.

Mol. Cryst. Liq. Cryst., Vol. 606: pp. 154–164, 2015

ISSN: 1542-1406 print/1563-5287 online
DOI: 10.1080/15421406.2014.905041

The Preparation and Characterization of New Antazoline Salts with Dicarboxylic Acids

AGNESE DRAVNIECE,[1,*] ANDRIS ACTIŅŠ,[1] KRISTĪNE KRŪKLE-BĒRZIŅA,[1] AND INESE SARCEVIČA[1,2]

[1]Faculty of Chemistry, University of Latvia, Riga, Latvia
[2]Latvian Institute of Organic Synthesis, Riga, Latvia

New antazoline salts with organic acids (fumaric acid, oxalic acid, and maleic acid) were prepared. The effect of the crystallization solvent and mechanochemical treatment on the crystalline forms of these salts was studied. Two polymorphs of antazoline hydrogen maleate were identified and their relative stability was determined. The molecular structures of antazoline hydrogen oxalate and antazoline hydrogen maleate showed differences in antazoline cation conformation. In crystal structures of all salts both imidazoline nitrogens of antazoline cation are involved in hydrogen bond formation with carboxyl groups of the acid.

Keywords Crystal structure; crystallization; hydrogen bonding motifs; polymorphism; salts; X-ray diffractometry

Introduction

Active pharmaceutical ingredients (APIs) typically contain functional groups that can form hydrogen bonds and therefore ensure the biological activity of the drugs [1, 2]. Many of these compounds are administered in the form of salts formed by interaction of organic bases and acids, provided that there is a sufficient difference between the acid and base pK_a values [3, 4]. For example, if the $\Delta pK_a > 3.75$ for pyridine ring containing compounds and carboxylic acids, then an ionic N–$H^+\cdots O^-$ bond will form [5]. Such molecular complexes as salts and cocrystals of APIs are desirable in the pharmaceutical industry because of extended patent protection and the different physicochemical properties compared to the parent drug [6–8]. Furthermore, the knowledge about crystalline forms of a drug compound offers additional information about its behaviour in the presence of other molecules. This information can be useful in the early stages of novel drug development.

Crystallization from solvents [9] and mechanical treatment [10] are some of the methods widely used in the preparation of new crystalline forms. The polymorph obtained by crystallization is often determined by the choice of the solvent [11, 12] and by the environmental conditions during the crystallization [13]. In addition, the crystals can contain solvent molecules and form solvates and hydrates [12].

*Address correspondence to Agnese Dravniece, Faculty of Chemistry, University of Latvia, Kr. Valdemara street 48, LV-1013, Riga, Latvia. E-mail: agnese.dravniece@lu.lv

Color versions of one or more of the figures in the article can be found online at www.tandfonline.com/gmcl.

Antazoline (*N*-(4,5-dihydro-1H-imidazol-2-ylmethyl)-*N*-(phenylmethyl)aniline) is an imidazoline derivative with anticholinergic properties that is used as an antihistamine drug for the treatment of nasal congestion and in eye drops [14]. It also has been proven to be effective in the treatment of cardiac arrhythmias [15, 16], and can be administered both intravenously and orally. Both antazoline hydrochloride and phosphate are used in pharmaceutical practice, yet new salts may offer an opportunity to improve drug properties as solubility, stability [17, 18]. In this study, preparation and characterization of new antazoline salts with fumaric acid, oxalic acid, and malonic acid is reported. Features of crystal and molecular structures of these salts are discussed.

Experimental

Materials

Antazoline base was prepared from antazoline phosphate (supplied by JSC Grindeks, Riga, Latvia). Sodium hydroxide, fumaric acid, oxalic acid dihydrate, maleic acid, and organic solvents were purchased from commercial sources and used as received. Water was deionized in the laboratory to $<0.1\ \mu$S.

Preparation of Antazoline Base

Antazoline base was prepared at ambient conditions by dissolving 10.00 g antazoline phosphate in 400 mL deionized water and mixing with an equimolar amount of 3.30 g sodium hydroxide dissolved in 25 mL deionized water. The resulting product was filtered, allowed to dry for 24 h, and stored in an airtight container.

Preparation of Antazoline Salts

Crystallization. Antazoline salts were prepared by dissolving 0.20 g of antazoline base in 10 mL of appropriate solvent (ethanol, 2-propanol, butanol, acetone, 2-butanone, 3-pentanone, ethyl acetate, butyl acetate, methanol, and tetrahydrofuran) and adding the chosen acid (0.04 g of fumaric acid, 0.10 g of oxalic acid dihydrate, or 0.09 g of maleic acid) dissolved in 10 mL of the same solvent. Experiments were conducted at 22°C, 40–60% RH. The resulting products were recovered by filtration and allowed to dry at ambient conditions for 1 h. The dried salts were kept in airtight containers.

Neat Grinding. Salts were also prepared by grinding 0.20 g of antazoline base with 0.04 g of fumaric acid, 0.07 g of oxalic or 0.09 g of maleic acid in a Retsch MM300 ball mill (Retsch GmbH) for 10 min with 15 Hz frequency without solvent addition. Mixture of starting compounds was milled in 35 mL grinding jars using one 1.5 cm stainless steel ball.

Polymorph Screening. Antazoline–dicarboxylic acid salts were suspended in various organic solvents (ethanol, 2-propanol, butanol, acetone, 2-butanone, 3-pentanone, ethyl acetate, butyl acetate, methanol, and tetrahydrofuran) at 22°C, 40–60% RH for 24 h, and the suspensions were allowed to dry. The composition of the product was determined using powder X-ray diffractometry.

Powder X-Ray Diffractometry

X-ray diffraction measurements were carried out with a Bruker D8 Advance X-ray powder diffractometer (Bruker AXS) equipped with a LynxEye position sensitive detector. Copper

radiation (CuK_α $\lambda = 1.5418$ Å) was used. The tube voltage and current were set to 40 kV and 40 mA. The divergence slit was 0.6 mm and the scattering slit was 8.0 mm. The samples were scanned over the 2θ range of 3–35° at the rate of 0.2 s/0.02°. The diffraction patterns were analyzed with DIFFRAC^{plus} EVA (ver. 2.1) software (Bruker AXS).

Single Crystal X-Ray Diffractometry

Single crystals of antazoline hydrogen oxalate (AO) and antazoline hydrogen maleate for structure determination were obtained from ethanol and acetone, respectively. Single crystal X-ray diffraction data were measured with a Nonius Kappa CCD diffractometer (Bruker AXS GmbH, Germany) with MoK_α radiation (0.71073 Å) at 173 K. Data reduction was performed with the DENZO/SCALEPACK software [19]. The crystal structures were solved by direct methods with Shelxs97 [20], refinement was performed using Shelxl97 [20].

Thermal Analysis

The thermal properties were investigated by DSC and DTA/TG.

DTA/TG analysis carried out on a SII Exstar 6000 DTA/TG6300 system. Powdered samples (5–10 mg) were analyzed on aluminum pans under air atmosphere at the heating rate of 10°C/min from 30°C to 200°C.

DSC was performed on a Mettler Toledo DSC 823e instrument. Samples (2–4 mg) were heated in aluminum pans under air atmosphere at the heating rate of 10°C/min from 40°C to 300°C.

Karl Fischer Titration

Karl Fischer titration was carried out using Metrohm Titrando 836. Approximately 300–500 mg of samples were weighed on a Precisa XB 220A balance and titrated with Hydranal Composite 5 (Fluka).

Results and Discussion

Crystalline Forms of Antazoline Salts

The pK_a values of antazoline are 7.79 and 9.74 [21, 22], while the pK_a values for fumaric acid are 3.03 and 4.44; for oxalic acid they are 1.25 and 4.14, and for maleic acid they are 1.9 and 6.07. The pK_a values suggest that salt formation is expected between antazoline and these acids. New salts of antazoline with oxalic acid, fumaric acid, and maleic acid were prepared during this study by crystallization and mechanical treatment. The formation of different crystalline forms of antazoline salts was investigated by suspending the salts in different solvents and by grinding in ball mills.

Antazoline Fumarate (AF)

Crystallization of antazoline with a fumaric acid (2:1 stoichiometry of acid to base) from all used solvents resulted in the formation of antazoline fumarate (AF) that became hydrated at ambient conditions. The comparison of PXRD patterns of AF, the hydrate ($AF{\cdot}0.5H_2O$), and the starting compounds is shown in Fig. 1. The stoichiometry of $AF{\cdot}0.5H_2O$ according

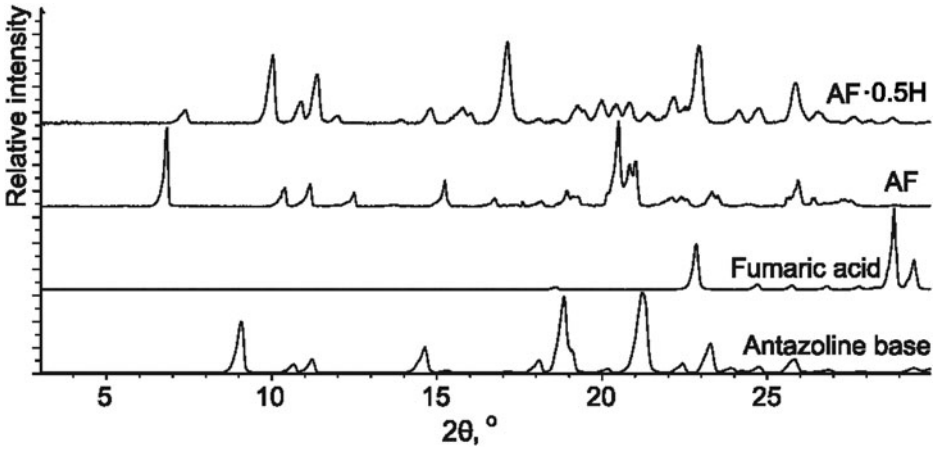

Figure 1. The PXRD patterns of antazoline base, fumaric acid, antazoline fumarate, and its hemihydrate.

to KF titration and DTA/TG analysis was 0.5 mol of water per 1 mol of AF. The dehydration of the AF·0.5H_2O occurred at 80°C and led to the anhydrous form (AF).

The search for antazoline fumarate polymorphs *via* slurrying in solvents did not produce new crystalline forms. Antazoline fumarate hemihydrate was obtained instead in all the slurrying experiments. The preparation of AF by milling antazoline base with fumaric acid in a ball mill without solvent addition resulted in AF.

Antazoline Hydrogen Oxalate (AO)

The crystallization of antazoline with oxalic acid from different solvents produced AO. The PXRD patterns of AO and starting materials are shown in Fig. 2. No new polymorphs were obtained in the experiments where AO was suspended in different solvents. Grinding antazoline base with oxalic acid dihydrate in a ball mill also produced AO.

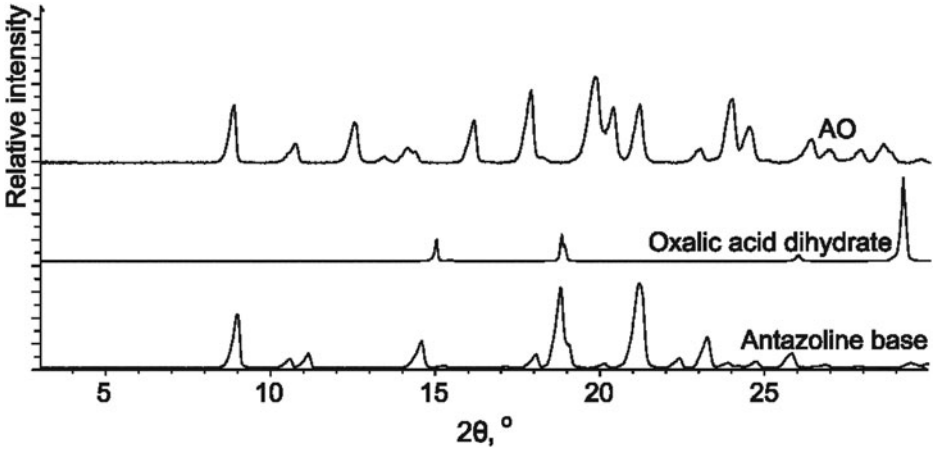

Figure 2. The PXRD patterns of antazoline, oxalic acid dihydrate, and AO.

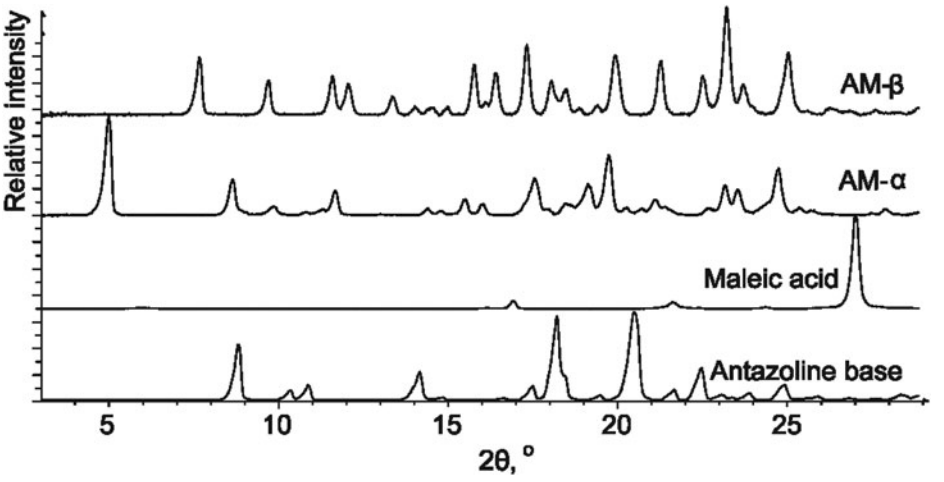

Figure 3. The PXRD patterns of antazoline, maleic acid, and AM polymorphs (AM-α and AM-β).

Antazoline Hydrogen Maleate (AM)

Crystallization from different solvents gave one nonsolvated form of antazoline hydrogen maleate (AM-α). Another polymorph of this salt (AM-β) was obtained by suspending the AM-α in isopropanol at ambient conditions. PXRD patterns of AM-α and AM-β are shown in Fig. 3. Both polymorphs were stable at room temperature, whereas during the storage at 100°C slow solid-state phase transition AM-$\alpha \rightarrow$ AM-β was observed.

The relative thermodynamic stability of both polymorphs was established by DSC analysis. The polymorphic system was monotropic, as the higher melting form (AM-β; melting point 154°C; heat of fusion 130.1 J g^{-1}) had a higher heat of fusion compared to the lower melting form (AM-α; melting point 151°C; heat of fusion 120.7 J g^{-1}). This monotropy suggested that the transition from AM-α to AM-β was irreversible as observed in the suspension experiment. The AM-α was the kinetic product and was prepared in the crystallization experiments, whereas grinding of antazoline base with maleic acid produced the thermodynamic product AM-β. An appropriate choice of the preparation method may therefore enable a control of polymorphic composition.

Crystal structures of AO and polymorphs of antazoline hydrogen maleate.

The crystal structures of AO, AM-α, and AM-β forms were determined in this work. AO and both polymorphs of AM crystallize in the triclinic crystal system with two formula units of the salt in the unit cell. The most relevant crystallographic data for AO, AM-α and AM-β are presented in Table 1.

The molecular structure of AO is shown in Fig. 4(b). Salt formation occurs by hydrogen transfer from oxalic acid to the N2 nitrogen of the antazoline imidazoline ring (Fig. 4(b)). A bifurcated hydrogen bond forms between the N3 nitrogen atom in the antazoline moiety and the O4 and O2 oxygen atoms in the oxalate monoanion. The imidazoline N2 nitrogen is hydrogen bonded through $N-H^{+}\cdots O^{\delta-}$ to the O3 oxygen in another oxalate anion (Table 2).

Oxalic moieties in AO are linked by shared H1 and H4A hydrogen atoms resulting in parallel chains perpendicular to the crystallographic axis *b* (Fig. 4(b)).

The molecular structures of AM both polymorphs are shown in Fig. 5.

Table 1. Crystallographic data for AO and hydrogen maleate polymorphs (AM-α and AM-β)

	AO	AM-α	AM-β
Formula	$C_{19}H_{21}N_3O_4$	$C_{21}H_{23}N_3O_4$	$C_{21}H_{23}N_3O_4$
Formula weight (g mol^{-1})	355.35	381.42	381.42
Crystal system	Triclinic	Triclinic	Triclinic
Space group	$P\bar{1}^{P\bar{1}}$	$P^{\bar{1}}$	$P^{\bar{1}}$
a (Å)	9.04000(10)	5.6341 (2)	7.4881(2)
b (Å)	9.8768(2)	10.1335 (2)	11.3146(2)
c (Å)	10.8307(2)	17.6670 (2)	11.9783(2)
α (°)	88.5578(6)	102.3221(12)	99.5695(12)
β (°)	67.4838(6)	90.6186(13)	103.767(13)
γ (°)	86.2971(10)	90.6706 (9)	91.9442(9)
V (Å^3)	891.45	985.27 (4)	969.08
Z	2	2	2
D_{calc} (g cm^{-3})	1.324	1.286	1.307
μ, mm^{-1}	0.094	0.090	0.092
$F(000)$	376	404	404
Number of parameters	245	293	262
Number of reflections ($I > 2\sigma$)	5779	2674	3529
wR	0.172	0.126	0.113
R ($I > 2\sigma$)	0.060	0.055	0.046
GOF	1.044	1.038	1.020
CCDC	975563	975562	975561

Table 2. Hydrogen bond parameters for antazoline molecular salts

D–H···A	D–H (Å)	H···A (Å)	D···A (Å)	<D–H···A (°)	Symmetry code
AO					
O1–H1···O1	1.23	1.23	2.4543(10)	180	1–x, –y, –z
N2–H2···O3	0.931(19)	1.912(19)	2.8145(13)	163.0(16)	x, 1+y, z
N3–H3···O2	0.93(2)	1.93(2)	2.8497(14)	173.4(17)	1+x, 1+y, z
N3–H3···O4	0.93(2)	2.505(19)	2.9994(13)	113.6(14)	1+x, 1+y, z
O4–H4A···N4	1.22	1.22	2.4481(10)	180	–x, –y, 1–z
AM- α					
N2–H2···O1	0.89(2)	1.94(2)	2.802(2)	161(2)	–1+x, –1+y, z
O3–H2B···O2	1.08(3)	1.34(3)	2.416(2)	176(3)	*intra*
N3–H3···O4	0.95(2)	1.83(2)	2.748(2)	162(2)	x, y, z
AM-β					
N2–H2···O1	0.875(17)	1.978(17)	2.8403(15)	168.2(16)	x, y, 1+z
O2–H2B···O3	1.20(2)	1.20(2)	2.4001(16)	178(2)	*intra*
N3–H3···O4	0.911(18)	1.858(18)	2.7257(17)	158.4(16)	x, y, z

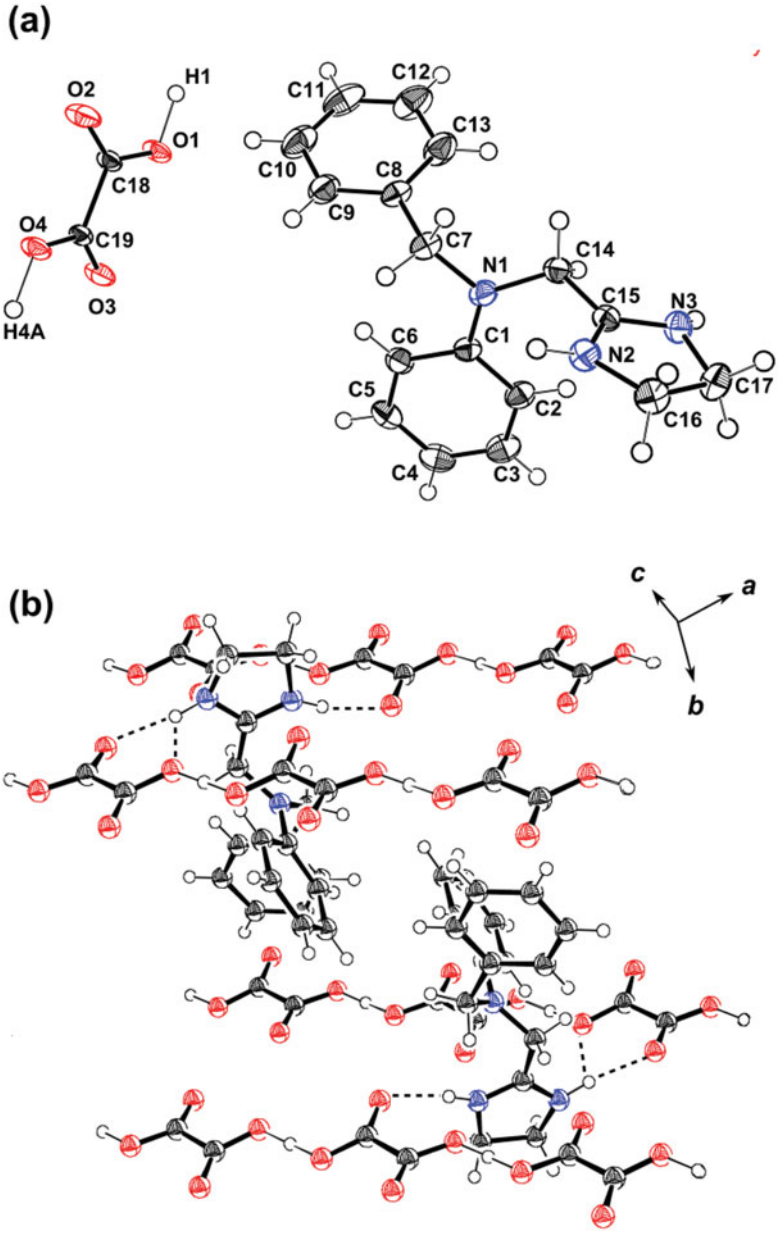

Figure 4. **(a)** The molecular structure of AO showing the numbering of atoms. **(b)** Hydrogen bonding motifs in AO. Thermal ellipsoids are drawn at the 50% probability level.

The benzyl group in AM-α was disordered over two positions with the occupancy factors of 0.6 (ring C8–C9–C10–C11A–C12A–C13A, black in Figure 5) and 0.4 (ring C8–C9–C10–C11B–C12B–C13B, grey in Fig. 5). The angle between these two possible ring positions is 27.9°. The angle between the plane of the maleate monoanion and the plane of the imidazoline ring in AM-α was 88.0°, while in AM-β this angle was 8.4°.

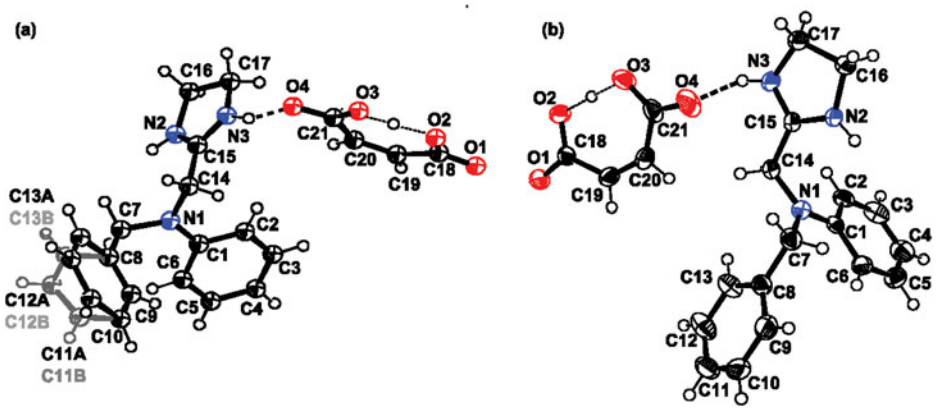

Figure 5. The molecular structures of antazoline hydrogen maleate showing the numbering of atoms in AM-α (a) and in AM-β (b). Thermal ellipsoids are drawn at the 50% probability level.

In the crystal structures of both AM polymorphs (AM-α and AM-β) similar hydrogen bonding motifs were observed. One of the carboxyl groups of the maleic acid was deprotonated. The remaining proton was involved in the formation of an intramolecular $O^{\delta-}\cdots H\cdots O^{\delta-}$ hydrogen bond with a graph set $S(7)$ between both carboxyl groups of the maleic acid. The protonated imidazoline nitrogen of the antazoline formed an ionic N^{+}–$H\cdots O^{\delta-}$ bond to the carboxylate group of the maleate monoanion. A neutral N–$H\cdots O$ hydrogen bond connected the other N of the antazoline imidazoline to the carbonyl O of the maleic acid carboxyl group. In both AM polymorphs, hydrogen-bonded acid and base moieties alternated to form extended parallel chains (Fig. 6).

The imidazoline ring in antazoline is prone to involvement in hydrogen bonding. The protonated N of antazoline in the base crystal structure acts as a proton donor for the nonprotonated N acceptor enabling the formation of an N–$H\cdots N$ hydrogen bond [22]. In salt structures, both of the imidazoline N atoms are H donors and involve in N–$H\cdots A$ (acceptor) hydrogen bonds. Although only one of the acid groups in dicarboxylic acids

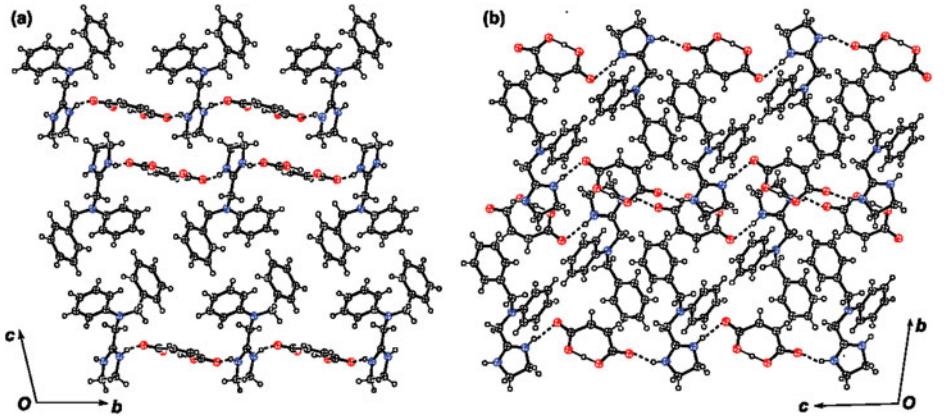

Figure 6. Packing diagrams showing hydrogen bonding motifs in the AM-α (a) and AM-β (b) crystal structure. For AM-α, only benzyl ring positions with occupancy 0.6 are shown.

Table 3. Torsion and dihedral angles of antazoline moiety in its crystalline forms

	Torsion angle (°)				Dihedral angle (°)		
Compound	C6–C1–N1–C7	N2–C15–C14–N1	C1–N1–C14–C15	C1–N1–C7–C8	Imidazoline/phenyl	Imidazoline/benzyl	Phenyl/benzyl
Antazoline base	−8.0(5)	19.7(5)	96.5(4)	96.0(4)	79.5	66.7	84.3
AO	3.4(2)	−33.3(1)	−77.9(1)	−75.6(1)	87.7	22.4	73.5
AM-α	−5.2(3)	24.0(3)	78.0(2)	97.5(2)	86.3	85.1*	73.9*
						67.4**	72.7**
AM-β	−2.0(1)	−1.8(2)	−88.4(2)	−75.0(2)	85.2	37.1	88.4

*Benzyl ring with occupancy of 0.6
**Benzyl ring with occupancy of 0.4

(oxalic, maleic acid) is deprotonated, both of them participate in hydrogen bonding as H acceptors. The ability of antazoline moiety to participate in H-bonding with both of its imidazole N leads to formation of infinite hydrogen-bonded chains in AM and AO.

The relative stability of polymorphs can be influenced by hydrogen bonding, packing forces, and other. The H···A (acceptor) distances in AM-α are slightly shorter than in AM-β (Table 2). However, there is a disorder of the benzyl ring position in AM-α probably resulting in an energy increase of this crystal structure. Furthermore, the crystallographic density of AM-β is larger than the density of AM-α (Table 1).

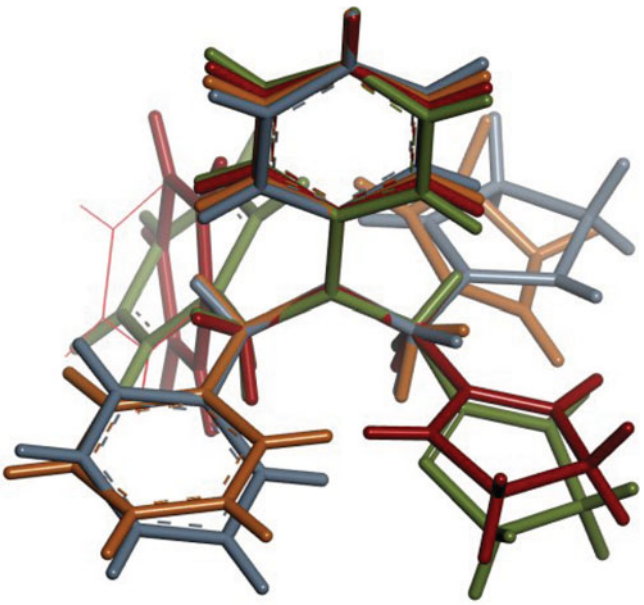

Figure 7. Conformational comparison of antazoline moiety in crystal structures of antazoline base (green), AO (blue), AM-α (red), and AM-β (orange).

To analyze conformation of antazoline moiety in its base [22] and salt crystal structures, torsion angles and dihedral angles between imidazoline, benzyl, and phenyl rings in antazoline cation have been compared (Table 3).

These angles show that the conformation of antazoline moiety is different in each crystalline form. The orientation of imidazoline and benzyl ring with regard to phenyl ring in AM-α crystal structure is similar to their orientation in the crystal structure of antazoline base, whereas the conformation of antazoline moiety in AM-β is more similar to that in AO (Fig. 7).

Conclusions

The antihistamine antazoline forms salts with dicarboxylic acids: fumaric acid, oxalic acid, and maleic acid were obtained by crystallization from solution and by grinding in ball mills. Two polymorphs of antazoline hydrogen maleate were obtained. Crystallization from solution produces the kinetically stable antazoline hydrogen maleate AM-α form while the thermodynamically stable AM-β form is obtained from grinding experiments.

The conformation of antazoline moiety in each crystal structure is different. However, similar trends can be observed between orientation of the benzyl and imidazoline rings with respect to the phenyl ring between antazoline base and AM-α and between AO and AM-β.

As a result of imidazoline N protonation in all antazoline salt crystal structures, both imidazole N participate in hydrogen bonding as hydrogen donors leading to characteristic acid–base–acid chain formation.

Funding

This work was supported by the European Regional Development Fund (No. 2011/0014/2DP/2.1.1.1.0/10/APIA/VIAA/092).

References

[1] Gancia, E., Montana, J. G., & Manallack, D. T. (2001). *J. Mol. Graphics Modell.*, *19*(3–4), 349.
[2] Hajduk, P. J., & Greer, J. (2007). *Nat. Rev. Drug Discover.*, *6*(3), 211.
[3] Childs, S. L., Stahly, G. P., & Park, A. (2007). *Mol. Pharm.*, *4*(3), 323.
[4] Mohamed, S., Tocher, D. A., Vickers, M., Karamertzanis, P. G., & Price, S. L. (2009). *Cryst. Growth Des.*, *9*(6), 2881.
[5] Bhogala, B. R., Basavoju, S., & Nangia, A. (2005). *Cryst. Eng. Comm*, *7*(90), 551.
[6] Guerrieri, P., Rumondor, A. C. F., Li, T., & Taylor, L. S. (2010). *AAPS Pharm. Sci. Tech.*, *11*(3), 1212.
[7] Blagden, N., de Matas, M., Gavan, P. T., & York, P. (2007). *Adv. Drug Delivery Rev.*, *59*(7), 617–630.
[8] Serajuddin, A. T. M. (2007). *Adv. Drug Delivery Rev.*, *56*, 603.
[9] Aaltonen, J., Allesø, M., Mirza, S., Koradia, V., Gordon, K. C., & Rantanen, J. (2009). *Eur. J. Pharm. Biopharm.*, *71*(1), 23.
[10] James, S. L., Adams, C. J., Bolm, C., Braga, D., Collier, P., Friščić, T., & Waddell, D. C. (2011). *Chem. Soc. Rev.*, *41*(1), 413.
[11] Gu, C. H., Li, H., Gandhi, R. B., & Raghavan, K. (2004). *Int. J. Pharm.*, *283*(1–2), 117.
[12] Morissette, S. L., Almarsson, O., Peterson, M. L., Remenar, J. F., Read, M. J., Lemmo, A. V., & Gardner, C. R. (2004). *Adv. Drug Delivery Rev.*, *56*(3), 275.
[13] Trask, A.V., Shan, N., Motherwell, W. D. S., Jones, W., Feng, S., Tan, R. B. H. *et al.* (2005). *Chem. Commun.*, *7*, 880.

[14] Figus, M., Fogagnolo, P., Lazzeri, S., Capizzi, F., Romagnoli, M., & Canovetti, A. (2011). *Eur. J. Ophthalmol.*, *20*(5), 811.
[15] Downar, E., & Waxman, M. B. (1975). *Medical Practice*, *113*(6), 391.
[16] Shah, S. S., Vaidya, C. H., & Doshi, H. V. (1972). *Postgrad. Med. J.*, *48*(559), 304.
[17] Elder, D. P., Holm, R., & Diego, H. L. (2013). *Int. J. Pharm.*, *453*, 88.
[18] Saal, C., & Becker, A. (2013). *Eur. J. Pharm. Sci.*, *49*(4), 614.
[19] Ostwinowski, Z., & Minor, W. (1997). In *Methods in Enzymology—Macromolecular Crystallography*, Carter, C. W. Jr. and Sweet, R. M. (Eds.), pp. 307–26, Academic Press: New York, Part A, 276.
[20] Sheldrick, G. M. (2008). *Acta Crystallogr., Sect. A: Found. Crystallogr.*, *A64*, 112.
[21] Parvez, M. (1997). *Acta Crystallogr., Sect. C: Cryst. Struct. Commun.*, *C53*, 506–508.
[22] Meloun, M., Syrový, T., & Vrána, A. (2004). *Talanta*, *62*(3), 511.